



Published in final edited form as:

*Mol Cancer Ther.* 2010 October ; 9(10): 2689–2699. doi:10.1158/1535-7163.MCT-10-0644.

## Maytansine and Cellular Metabolites of Antibody-Maytansinoid Conjugates Strongly Suppress Microtubule Dynamics by Binding to Microtubules

Manu Lopus<sup>1</sup>, Emin Oroudjev<sup>1</sup>, Leslie Wilson<sup>1</sup>, Sharon Wilhelm<sup>2</sup>, Wayne Widdison<sup>2</sup>, Ravi Chari<sup>2</sup>, and Mary Ann Jordan<sup>1</sup>

<sup>1</sup> Department of Molecular, Cellular, and Developmental Biology, and the Neuroscience Research Institute, University of California, Santa Barbara, CA 93106

<sup>2</sup> ImmunoGen, Inc, 830 Winter Street, Waltham, MA 02451

### Abstract

Maytansine is a potent microtubule-targeted compound that induces mitotic arrest and kills tumor cells at sub-nanomolar concentrations. However, its side effects and lack of tumor specificity have prevented successful clinical use. Recently, antibody-conjugated maytansine derivatives have been developed to overcome these drawbacks. Several conjugates show promising early clinical results. We evaluated the effects on microtubule polymerization and dynamic instability of maytansine and two cellular metabolites (S-methyl DM1 and S-methyl DM4) of antibody-maytansinoid conjugates that are potent in cells at pM levels and that are active in tumor-bearing mice. Although S-methyl DM1 and S-methyl DM4 inhibited polymerization more weakly than maytansine, at 100 nmol/L they suppressed dynamic instability more strongly than maytansine (by 84% and 73%, respectively, compared with 45% for maytansine). However, unlike maytansine, S-methyl DM1 and S-methyl DM4 induced tubulin aggregates detectable by electron microscopy at concentrations  $\geq 2$   $\mu\text{mol/L}$ , with S-methyl DM4 showing more extensive aggregate formation than S-methyl DM1. Both maytansine and S-methyl DM1 bound to tubulin with similar  $K_D$ 's ( $0.86 \pm 0.2$   $\mu\text{mol/L}$  and  $0.93 \pm 0.2$   $\mu\text{mol/L}$ , respectively). Tritiated S-methyl DM1 bound to 37 high affinity sites per microtubule ( $K_D$ ,  $0.1 \pm 0.05$   $\mu\text{mol/L}$ ). Thus, S-methyl DM1 binds to high affinity sites on microtubules 20-fold more strongly than vinblastine. The high affinity binding is likely at microtubule ends and is responsible for suppression of microtubule dynamic instability. Also, at higher concentrations, S-methyl DM1 showed low affinity binding either to a larger number of sites on microtubules or to sedimentable tubulin aggregates. Overall, the maytansine derivatives that result from cellular metabolism of the antibody conjugates are themselves potent microtubule poisons, interacting with microtubules as effectively as or more effectively than the parent molecule.

### Keywords

Maytansine; Microtubules; Dynamic Instability; Cancer Chemotherapy; Vinblastine

## Introduction

Maytansine (Fig. 1) is a 19-member ansa macrolide structure attached to a chlorinated benzene ring (1). It was originally isolated from the shrub *Maytenus ovatus* (2). The antimetabolic effect of maytansine has been attributed to its ability to inhibit microtubule assembly by binding to tubulin with a  $K_D$  of  $\sim 1 \mu\text{mol/L}$ , at or near the vinblastine-binding site (3–5). Maytansine is effective *in vivo* against Lewis lung carcinoma and B16 murine melanocarcinoma solid tumors, and has antileukemic activity against P388 murine lymphocytic leukemia (6). The microtubule-targeted antiproliferative activity of maytansine was substantiated in a screening of 60 human cancer cell types by the U.S. National Cancer Institute (6). Although maytansine inhibits microtubule assembly and kills cancer cells, its utility in the clinic has been hampered by severe side effects and poor efficacy (6). When evaluated as a single agent, maytansine failed to show any significant response in patients with different types of cancers (6,7).

Recent development of maytansine analogs conjugated to antibodies to increase their target specificity has revived interest in these compounds as potential drugs for cancer chemotherapy (6,8–10). The present study focuses on the effects of maytansine and its thiomethyl derivatives, S-methyl DM1 and S-methyl DM4 (Fig. 1) that are the primary cellular or liver metabolites of antibody-maytansinoid conjugates prepared with thiol-containing maytansinoids DM1 and DM4, respectively. Antibody conjugates of DM1 and DM4 kill several types of cancer cells in the nanomolar to picomolar concentration range (10,11). Importantly, a recent Phase II clinical trial with the maytansinoid conjugate, trastuzumab-DM1, has shown promise yielding an interim overall response rate of 39% in patients with metastatic breast cancer (12). Inside cells, maytansinoid conjugates undergo lysosomal degradation, and the proteolytic digestion of the antibody component of the conjugates gives rise to a number of metabolites (10), that may constitute active drugs. Although maytansine's binding to tubulin and its effects on microtubule assembly have been studied, its effects on microtubule dynamic instability are unknown. In addition, the mechanisms of action of the metabolites of the antibody conjugates, which may ultimately constitute the active intracellular components, are unknown.

Microtubules are dynamic cytoskeletal polymers that switch stochastically between states of growing and shortening, called "dynamic instability" (13). They function in the precise segregation of chromosomes during cell division, transport of cellular cargos, and positioning and movement of intracellular organelles (13,14). Inhibition of microtubule function leads to cell cycle arrest and cell death (14). Microtubule-targeted drugs including the Vinca alkaloids, taxanes, and epothilones suppress the dynamic instability of microtubules, induce mitotic arrest, inhibit cell proliferation and induce apoptosis (15). In this study, we evaluated the effects of maytansine and its two thiomethyl-containing derivatives S-methyl DM1 and S-methyl DM4 on microtubule dynamic instability, and we determined the binding of S-methyl DM1 to tubulin and microtubules.

Although S-methyl DM1 and S-methyl DM4 inhibited microtubule assembly more weakly than maytansine, they suppressed dynamic instability more strongly than maytansine. Like vinblastine, the maytansinoids potently suppress microtubule dynamic instability by binding to a small number of high affinity sites, most likely at microtubule ends. Thus, the maytansine derivatives that result from cellular metabolism of the antibody conjugates are themselves potent microtubule poisons, interacting with microtubules as effectively as or more effectively than the parent molecule.

## Materials and Methods

### Synthesis and Chemistry

The thiol-containing maytansinoids DM1 [*N*<sup>2'</sup>-deacetyl-*N*<sup>2'</sup>-(3-mercapto-1-oxopropyl)-maytansine] and DM4 [*N*<sup>2'</sup>-deacetyl-*N*<sup>2'</sup>-(4-mercapto-4-methyl-1-oxopentyl)-maytansine] were synthesized as previously described (16). Each of these compounds was converted to its respective thiomethyl derivative, S-methyl DM1 [*N*<sup>2'</sup>-deacetyl-*N*<sup>2'</sup>-(3-thiomethyl-1-oxopropyl)-maytansine] and S-methyl DM4 [*N*<sup>2'</sup>-deacetyl-*N*<sup>2'</sup>-(4-thiomethyl-4-methyl-1-oxopentyl)-maytansine] by reacting them overnight with an excess of methyl iodide and *N,N*-diisopropylethylamine in a solution of *N,N*-dimethylformamide (DMF). The resulting S-methylated derivatives, S-methyl DM1 and S-methyl DM4 were purified by reverse-phase preparatory HPLC eluting with a linear gradient of acetonitrile in deionized water. The purity and identity of each isolated compound were assessed by HPLC and mass spectroscopy. [<sup>3</sup>H] DM1 was synthesized as previously described (17) and converted to [<sup>3</sup>H] S-methyl DM1 by methylation with methyl iodide as described for S-methyl DM1 above.

### Purification of Tubulin and Microtubule Protein

Bovine brain microtubule protein (MTP, tubulin and microtubule-associated proteins (MAPs)) was isolated by two cycles of temperature-dependent polymerization and depolymerization (18). Tubulin was purified from MTP by phosphocellulose chromatography (19), and concentrated to 9 mg/mL in 100 mmol/L Pipes (1,4-piperazinediethanesulfonic acid), 1 mmol/L EGTA, and 1 mmol/L MgSO<sub>4</sub>, pH 6.8 (PEM buffer) at 30 °C. Purified tubulin was drop-frozen in liquid nitrogen, and stored at -70 °C until use. Protein concentration was determined by the method of Bradford using bovine serum albumin as the standard (20).

### Effects of the Maytansinoids on Microtubule Polymerization

The ability of maytansine, S-methyl DM1 and S-methyl DM4 to inhibit microtubule assembly was determined by incubating MTP (3 mg/mL) with a range of maytansinoid concentrations (0 – 20 μmol/L) in the presence of 1 mmol/L GTP in PEM buffer (30°C, 45 min). For sedimentation assays, the polymers formed were centrifuged (35000 × *g*, 1 h, 30°C). The microtubule pellets were depolymerized at 0°C overnight and the protein concentrations determined (20). The sedimentation assay for each compound was performed at least twice (21). For observing microtubule morphology, samples were fixed in 0.2% glutaraldehyde, and stained with 0.5% uranyl acetate (21). The images were acquired at 50000 × or 100000 × magnification using a JEOL 1230 transmission electron microscope at 80 KV.

### Effects of Maytansine and Its Derivatives on Microtubule Dynamic Instability

Microtubule dynamic instability parameters were measured as previously described (22). Briefly, tubulin (1.5 mg/mL) was assembled on the ends of sea urchin (*Strongylocentrotus purpuratus*) axoneme fragments at 30°C in 87 mmol/L Pipes, 36 mmol/L Mes, 1.4 mmol/L MgCl<sub>2</sub>, 1 mmol/L EGTA, pH 6.8 (PMME buffer) containing 2 mmol/L GTP for 30 min to achieve steady state. We used a 100 nmol/L concentration of each compound, to analyze their individual effects on dynamic instability. Time-lapse images of microtubule plus ends were obtained at 32°C by video-enhanced differential interference contrast microscopy using an Olympus IX71 inverted microscope with a 100 × (NA = 1.4) oil immersion objective. We identified plus ends of the microtubules by their faster growth rate, greater length changes, and larger number of microtubules per axoneme end as compared with the minus ends (22). Microtubule dynamics were recorded for 40 min at 30°C, capturing 10 min long videos for each area under observation. The rates and durations of growing and shortening and the transition frequencies were determined after tracking the microtubules using RTM-II software (23) and analyzing using IgorPro software (MediaCybernetics, Bethesda, MD). Microtubules

were considered as growing if they increased in length  $>0.3 \mu\text{m}$  at a rate  $>0.3 \mu\text{m}/\text{min}$ . Shortening events were identified by a  $>1 \mu\text{m}$  length reduction at a rate  $>2 \mu\text{m}/\text{min}$ . Fifteen to 25 microtubules were analyzed per condition. The catastrophe (a transition from a growing or attenuated state to shortening) frequency was calculated as the total number of catastrophes divided by time spent growing and attenuated (paused). The rescue (transition from shortening to growing) frequency was calculated as the total number of rescue events divided by total time spent shortening. The dynamicity of microtubules was derived as the sum of the total growth length and the total shortening length divided by the total time.

### Binding of Maytansine or S-methyl DM1 to Soluble Tubulin

Maytansine or S-methyl DM1 (0–20  $\mu\text{mol}/\text{L}$ ) was incubated with 3  $\mu\text{mol}/\text{L}$  tubulin in PEM buffer for 45 min at 30°C. The relative intrinsic fluorescence intensity of tubulin was monitored at 335 nm in a Perkin Elmer LS 50B spectrofluorometer (Waltham, MA) using a 0.3-cm path length cuvette at an excitation wavelength of 295 nm. The fluorescence emission intensity of S-methyl DM1 and maytansine at this excitation wavelength was negligible. The inner filter effects were corrected using the formula  $F_{\text{corrected}} = F_{\text{observed}} \cdot \text{antilog} [(A_{\text{ex}} + A_{\text{em}})/2]$ , where  $A$  is the absorbance at the excitation wavelength and  $A_{\text{em}}$  is the absorbance at the emission wavelength. The dissociation constant ( $K_D$ ) was determined by the formula:  $1/a = K_D/[ \text{free ligand} ] + 1$ , where  $a$  is the fractional occupancy of the drug and  $[ \text{free ligand} ]$  is the concentration of free maytansine or S-methyl DM1. The fractional occupancy ( $a$ ) was determined by the formula  $a = \Delta F/\Delta F_{\text{max}}$ , where  $\Delta F$  is the change in fluorescence intensity when tubulin and its ligand are in equilibrium and  $\Delta F_{\text{max}}$  is the value of maximum fluorescence change when tubulin is completely bound with its ligand (24). Experiments were performed three times.

### Stoichiometry of S-methyl DM1 Binding to Steady-State Microtubules

MTP (3 mg/mL) was polymerized to steady state in PEM buffer and then different concentrations of [ $^3\text{H}$ ]S-methyl DM1 (0–4  $\mu\text{M}$ , SA =145 mCi/mmol) were added at 30°C, and incubated for 1 h. Microtubules were centrifuged at  $35000 \times g$  (1 h, 30°C) through a 0.5 mL glycerol/DMSO cushion (30% glycerol: 10% DMSO). After centrifugation, the supernatant and the cushion were aspirated, and the drug bound to the side of the tubes was carefully removed by overlaying the pellet with 50% glycerol and subsequently aspirating the glycerol from the pellet. The pellets were dissolved in water at 0°C overnight; the protein was measured by Bradford assay; binding to microtubules was determined after addition to Ready Protein liquid scintillation cocktail (Beckman Coulter, Fullerton, CA) in a Beckman LS1801 Scintillation Counter. The mean lengths of microtubules in the presence and absence of S-methyl DM1 were determined by electron microscopy (25). Samples were taken at steady state in the presence or absence of S-methyl DM1, fixed in 0.2% glutaraldehyde, and stained with 0.5% uranyl acetate. The images were acquired at  $3000 \times$  magnification using a JEOL 1230 transmission electron microscope at 80 KV for microtubule length measurements (21). From the lengths of microtubules, the amount of the pelleted protein, and the specific activity of [ $^3\text{H}$ ]S-methyl DM1, the binding stoichiometry of S-methyl DM1 to microtubules was determined. The  $K_D$  for microtubule–S-methyl DM1 interaction was determined as the negative inverse slope of a Scatchard plot of the binding data (26).

## Results

### Inhibition of Microtubule Polymerization by Maytansine and its Thiomethyl Analogs

To determine if the thiomethyl analogs of maytansine (the metabolites) retained the basic microtubule-targeted effects of maytansine, we compared the abilities of S-methyl DM1 and S-methyl DM4 to inhibit microtubule polymerization with that of maytansine. Microtubule protein (3 mg/mL) was assembled in the presence or absence of a range of maytansinoid concentrations (0–20  $\mu\text{mol}/\text{L}$ , 30°C, 1 h) and the mass of polymer was determined by

sedimentation (Materials and Methods). Under the experimental conditions used, the half-maximal concentration for inhibition of microtubule assembly for maytansine was  $1 \pm 0.02$   $\mu\text{mol/L}$ ; for S-methyl DM1,  $4 \pm 0.1$   $\mu\text{mol/L}$ ; and for S-methyl DM4,  $1.7 \pm 0.4$   $\mu\text{mol/L}$  (Fig. 2A). Maytansine showed nearly complete inhibition of microtubule polymerization at 3  $\mu\text{mol/L}$ . S-methyl DM1 required a concentration of 20  $\mu\text{mol/L}$  to show a similar effect on polymer mass. S-methyl DM4 did not show complete inhibition of polymer mass. Instead, a plateau at 75% inhibition of polymerization was reached between 10  $\mu\text{mol/L}$  and 20  $\mu\text{mol/L}$  (Fig. 2A). By electron microscopy, we imaged the polymers formed in the absence or presence of a range of concentrations (0.1  $\mu\text{mol/L}$ , 2  $\mu\text{mol/L}$ , 4  $\mu\text{mol/L}$ , and 20  $\mu\text{mol/L}$ ) of maytansine, S-methyl DM1, and S-methyl DM4. At 0.1  $\mu\text{mol/L}$ , the microtubules were intact no detectable aggregates for all three compounds. Maytansine (2  $\mu\text{mol/L}$ ) nearly completely inhibited tubulin assembly, showing very few microtubules and no aggregates (images not shown). At higher maytansine concentrations (4  $\mu\text{mol/L}$  and 20  $\mu\text{mol/L}$ ), there were no microtubules or aggregates (images not shown). In contrast, with S-methyl DM1 (2  $\mu\text{mol/L}$ ), there was a small number of small aggregates along with the microtubules. At 20  $\mu\text{mol/L}$ , S-methyl DM1 showed an increase in aggregate formation. Microtubules predominated, but large aggregates like those shown in Fig 2B were also observed frequently. Specifically, we observed 2 or 3 of the structures shown in Figure 2B per 150 mesh grid square. S-methyl DM4 was the most potent inducer of aggregates. At 2  $\mu\text{mol/L}$  S-methyl DM4, we observed aggregates as well as both normal and also some imperfect, ragged microtubules with loose protofilamentous structure (Fig 2B). At 20  $\mu\text{mol/L}$  S-methyl DM4, more extensive aggregation of tubulin occurred with no intact microtubules (Fig 2B), suggesting that that the plateau observed at higher S-methyl DM4 concentration was due to the formation of aggregates.

### Suppression of Microtubule Dynamic Instability by the Maytansinoids

We analyzed the effects of maytansine, S-methyl DM1 and S-methyl DM4 on the dynamic instability parameters of individual, reassembled MAP-free bovine brain microtubules at their plus ends at steady state. Microtubule growth and shortening occurred predominantly at the plus ends under the conditions used (Materials and Methods). Life history traces over time showing the changes in length of individual microtubules in the absence and presence of 100 nmol/L maytansinoid are shown in Fig. 3. We used the life history traces to determine the dynamic instability parameters shown in Table 1. Control microtubules displayed typical growth and shortening dynamics (Figure 3A), while incubation with 100 nmol/L maytansine (Fig. 3B), S-methyl DM1 (Fig. 3C), or S-methyl DM4 (Fig. 3D) clearly suppressed dynamic instability. Specifically, all the maytansine analogs suppressed the growing and shortening rates and increased the fraction of time in the attenuated state. The plus ends of control microtubules grew slowly at a mean rate of  $1.7 \pm 0.2$   $\mu\text{m/min}$ , shortened rapidly at a mean rate of  $8.9 \pm 0.8$   $\mu\text{m/min}$  and occasionally persisted in an attenuated or paused state, neither growing nor shortening detectably (Table 1). Maytansine (100 nmol/L) significantly reduced both the growth and the shortening lengths (by ~40%) and the growth and shortening rates by 35%. Dynamicity, a measure of the overall addition and loss of tubulin at the microtubule ends per unit time, was suppressed by 45% by 100 nmol/L maytansine.

Interestingly, the thiomethyl maytansinoids were significantly more potent than maytansine in suppressing the dynamic instability of microtubules. For example, S-methyl DM1 showed very strong suppression of dynamic instability, significantly suppressing the shortening rate by 70%, the shortening length by 60%, the catastrophe frequency by 90% and the dynamicity by 84% (Table 1). This is compared with suppression of the same parameters by maytansine by only 35%, 40%, 30%, and 45%, respectively. The other maytansinoid analog, S-methyl DM4, affected the dynamic instability parameters in a similar manner to S-methyl DM1, suppressing the same parameters by 56%, 60%, 90%, and 73%, respectively. Moreover, S-methyl DM1 and S-methyl DM4 increased the percentage of time microtubules remained in a state of

attenuated dynamic instability (pause) by 41% and 30%, respectively, whereas maytansine had a negligible effect on the pause state.

### Maytansine and S-methyl DM1 Bind to Soluble Tubulin

Using the changes in the intrinsic tryptophan fluorescence of tubulin as a probe for ligand binding, we studied the binding of maytansine and S-methyl DM1 to tubulin. When excited at 295 nm, increasing concentrations of maytansine (0.5–20  $\mu\text{mol/L}$ ) or S-methyl DM1 (1–8  $\mu\text{mol/L}$ ) showed increasing quenching of tubulin fluorescence, indicating that both maytansinoids bind to tubulin. Analysis of the inverse fractional receptor occupancy of maytansine versus the inverse of the free maytansine concentration gave an equilibrium dissociation constant ( $K_D$ ) of  $0.86 \pm 0.23 \mu\text{mol/L}$  (Fig. 4A). Similar analysis of S-methyl DM1 gave a  $K_D$  of  $0.93 \pm 0.22 \mu\text{mol/L}$  (Fig. 4B), indicating that both compounds bind relatively strongly to soluble bovine brain tubulin.

### S-methyl DM1 Binds to a Small Number of High-Affinity Sites at Microtubule Ends

To gain understanding into the molecular mechanism underlying the suppression of dynamic instability by the maytansinoids, the binding of S-methyl DM1 to steady state microtubules was investigated using [ $^3\text{H}$ ]S-methyl DM1. As described in detail in Materials and Methods, tubulin with MAPs (3 mg/mL) was polymerized to steady state after which a range of concentrations of radiolabeled S-methyl DM1 was added and incubation continued for 1 h. The microtubules and any large sedimentable polymers were collected by centrifugation through a glycerol/DMSO stabilizing cushion. The sedimented protein and the associated radioactivity were determined and the lengths of the microtubules were measured by electron microscopy. Under these conditions, the mean length of the microtubules remained relatively constant (14.4–14.5  $\mu\text{m}$  with a maximum standard deviation of 4  $\mu\text{m}$  at all concentrations between 0 and 100 nmol/L S-methyl DM1 and 13.9–14.1  $\mu\text{m}$  with standard deviation of 4.5  $\mu\text{m}$  at 500 nmol/L – 4  $\mu\text{mol/L}$  S-methyl DM1). The mean microtubule lengths were factored into the stoichiometry calculation (drug bound per microtubule) for all concentrations. Under the conditions of the experiment (pre-assembled MAP-rich microtubules incubated with S-methyl DM1 for only one hour), the microtubule polymer mass decreased less than 4% at any of the maytansinoid concentrations. S-methyl DM1 bound to microtubules in a concentration-dependent manner, and the number of maytansinoid molecules bound per microtubule at various concentrations is shown in Fig. 5 and Supplementary Data Table 1. For example, at 0.1  $\mu\text{mol/L}$ , the concentration of S-methyl DM1 that suppressed dynamicity by 84% (Table 1),  $19 \pm 1$  S-methyl DM1 molecules were bound per microtubule (Fig 5A). Scatchard analysis (microtubule-bound S-methyl DM1/free S-methyl DM1 versus microtubule-bound S-methyl DM1) indicated that S-methyl DM1 has two types of binding sites on the microtubules or sedimentable aggregates, saturable high affinity sites and low affinity sites (Fig. 5B). The equilibrium dissociation constant for S-methyl DM1–microtubule interaction at low drug concentrations (10 nmol/L – 100 nmol/L) was 0.1  $\mu\text{mol/L}$ . However, at higher drug concentrations, (0.1  $\mu\text{mol/L}$  to 4  $\mu\text{mol/L}$ ) the binding of S-methyl DM1 to microtubules and sedimentable aggregates that may have been present at higher concentrations showed a second slope that was not saturated even at 4  $\mu\text{mol/L}$ ; at this concentration  $210 \pm 37$  molecules of S-methyl DM1 were bound per microtubule or sedimentable aggregate. Thus, from the X-intercept of Fig. 5C and inverse slope, S-methyl DM1 appears to bind to 37 high affinity sites on microtubules with a  $K_D$  of  $0.1 \pm 0.05 \mu\text{mol/L}$  and to a large number of low affinity sites on microtubules and sedimentable aggregates with a  $K_D$  of  $2.2 \pm 0.2 \mu\text{mol/L}$  (Fig. 5C).

## Discussion

We have examined the molecular mechanisms of action of maytansine and its thiomethyl-containing derivatives, S-methyl DM1 and S-methyl DM4, on purified microtubules *in vitro*.

The thiomethyl-containing derivatives were chosen because they represent stable derivatives of the thiol-containing maytansinoids DM1 and DM4 that were used in the preparation of antibody-maytansinoid conjugates and that are currently in clinical evaluation. In addition, these derivatives are the main cellular metabolites of the conjugates and thus may indeed represent the active cytotoxic agents (10).

Inhibition of microtubule assembly by maytansine showed a steep concentration dependence, exhibited the most potent inhibition ( $IC_{50}$ ,  $1 \pm 0.02 \mu\text{mol/L}$ ), and induced no formation of aggregates when examined by electron microscopy. In contrast, the two thiomethyl derivatives exhibited shallow concentration-dependent inhibition gradients, somewhat higher  $IC_{50}$ 's, 1.7 and  $4 \mu\text{mol/L}$  (Fig. 2A), and induced tubulin aggregate formation. S-methyl DM1 induced some small aggregates, particularly at high concentrations ( $20 \mu\text{mol/L}$ ) whereas S-methyl DM4 induced formation of large, very extensive aggregates (Figure 2B), at concentrations  $\geq 2 \mu\text{mol/L}$ , resulting in a plateau in the concentration-dependence for the quantity of sedimentable polymer at 25% of the control polymer mass between 10 and  $20 \mu\text{mol/L}$ . However, at  $100 \text{ nmol/L}$ , the concentration at which effects on dynamic instability were measured, none of the compounds induced detectable tubulin aggregation.

We examined the interactions of maytansine and S-methyl DM1 with soluble tubulin. Maytansine decreased the intrinsic tryptophan fluorescence of tubulin in a concentration-dependent manner (Fig. 4A). Assuming a single binding site for maytansine on tubulin, linear regression of the data yielded an apparent equilibrium dissociation constant ( $K_D$ ) of  $0.86 \pm 0.2 \mu\text{mol/L}$ , similar to the  $K_D$  of  $0.7 \mu\text{mol/L}$  reported previously (4). Similar analysis using S-methyl DM1 resulted in a  $K_D$  of  $0.93 \pm 0.2 \mu\text{mol/L}$  (Fig. 4B), indicating that both maytansine and its derivative bind to soluble tubulin with relatively high affinity.

We also investigated the binding of S-methyl DM1 to microtubules pre-assembled from purified MAP-rich tubulin. [ $^3\text{H}$ ]S-methyl DM1 bound to the microtubules in a concentration-dependent manner (Fig. 5A, and Supplementary Data Table 1). At  $100 \text{ nmol/L}$ , a concentration that showed strong (84%) suppression of dynamic instability, 19 molecules of S-methyl DM1 were bound per microtubule. At  $1 \mu\text{mol/L}$  and  $4 \mu\text{mol/L}$  S-methyl DM1, approximately 105 and 210 molecules of S-methyl DM1 were bound per microtubule or to the relatively rare sedimentable aggregates, respectively. Scatchard analysis of the binding of S-methyl DM1 indicated two types of binding sites for this maytansinoid, 37 saturable high affinity sites per microtubule with an apparent  $K_D$  of  $0.1 \pm 0.05 \mu\text{mol/L}$ , and several hundred low affinity sites (Fig. 5B, C) with a 20-fold higher  $K_D$ . The affinity of S-methyl DM1 for the 37 high affinity sites on the microtubule is 9-fold greater than its affinity for soluble tubulin ( $K_D$ ,  $0.9 \mu\text{mol/L}$ ). The low number of very high affinity binding sites and the strong suppression of dynamic instability events occurring at microtubule ends (catastrophe, rescue, and shortening) (Table 1) suggest that S-methyl DM1 potently suppresses dynamic instability through binding to tubulin at the ends of microtubules, which have approximately 13 subunits exposed at each end. The number of high affinity binding sites is only slightly higher than the number of exposed subunits at the two ends. The reasons for the unusual number of 37 binding sites per microtubule (as compared with  $16.8 \pm 4.3$  high affinity binding sites for vinblastine and  $14.7 \pm 1.3$  for eribulin (27,28)) may be due to possible binding at both microtubule ends, slight fraying at microtubule ends resulting in exposure of additional binding sites, or the presence of very small maytansinoid-tubulin oligomers at the microtubule ends (discussed further below).

### Suppression of Dynamic Instability by Maytansinoids

Microtubule-targeted agents inhibit cancer cell proliferation by arresting cells at mitosis and inducing them to undergo programmed cell death (15). Many of these agents do so by suppressing microtubule dynamics at concentrations well below those required to alter microtubule polymer mass (14,15). We assessed the effect of maytansine, S-methyl DM1, and

S-methyl DM4 at a concentration of 100 nmol/L on the dynamic instability of microtubules. At this concentration, S-methyl DM1 and S-methyl DM4 reduced the microtubule polymer mass by less than 3% and maytansine reduced it by 20% (Fig. 2A). A lower concentration of 20 nmol/L S-methyl DM1 was also examined and showed minimal suppression of dynamicity (~6% change) (data not shown) indicating that 100 nmol/L was in the appropriate concentration range to assess the effects of the compound on dynamic instability. All three compounds suppressed dynamic instability. Maytansine, like vinblastine and estramustine (28,29), suppressed both the growing and the shortening rates to similar extents (35%) and the catastrophe and rescue frequencies similarly (30% and 40%, respectively). In contrast, the thiomethyl derivatives suppressed the rate of shortening more strongly (56–70%) than the rate of growing (~24%) and they suppressed the catastrophe frequency (by 90%) significantly more strongly than the rescue frequency (by only 44–50%). Among the maytansinoids tested, S-methyl DM1 most strongly suppressed the dynamicity followed by S-methyl DM4 > maytansine (Table 1). Thus, S-methyl DM1 and S-methyl DM4 both stabilize microtubules more strongly than maytansine. Although no aggregates were detected at the concentration at which effects on dynamic instability were measured, it is reasonable to consider that at 100 nmol/L, the maytansine derivatives may have induced formation of very small, undetected aggregates consisting of from two to a few tubulin dimers, either in solution or at the microtubule ends. Such tightly-associated drug-tubulin complexes may have effectively capped the microtubule ends, thus inhibiting loss of tubulin from the ends and preferentially inhibiting catastrophe and shortening events, and the resultant dynamicity. Thus, they may be responsible for the stronger suppression of microtubule dynamics by S-methyl DM1 and S-methyl DM4 than by maytansine. Aggregated tubulin dimers may also be responsible for the enhanced number of S-methyl DM1 molecules bound to sedimentable polymer at concentrations  $\geq 500$  nmol/L (60–210 molecules per microtubule) (Supplementary Table 1).

### Mechanism of Suppression of Microtubule Dynamic Instability by Maytansine and Its Derivatives

**Mechanism of Suppression of the Growing Rate**—Maytansine and its derivatives suppressed the growing rate of microtubules at 100 nmol/L (Table 1). One possibility is that the suppression of the growing rate is due to a decrease in the association rate constant for tubulin addition. Microtubule growth rate is represented as:

$$R_g = K_+ C - K_- \quad (1)$$

where the growing rate,  $R_g$ , depends on the association rate constant ( $K_+$ ), the dissociation rate constant ( $K_-$ ), and the concentration of soluble tubulin ( $C$ ) (30). As  $C$  was not affected by low drug concentrations (100 nmol/L), only a reduction in  $K_+$  or an increase in  $K_-$  could contribute to the reduction in the growing rate. Because each of the compounds strongly suppressed the shortening rate also, there was no increase in  $K_-$ . Thus, we suggest that a decrease in the association rate constant for tubulin due to the binding of the compound at the tips of microtubules was responsible for suppressing the growing rate. Moreover, the propensity of maytansine to inhibit GTP exchange of soluble tubulin (31–33) might also have contributed to the decrease in  $K_+$  and thereby, suppression of the growth rate.

**Mechanism of Suppression of the Shortening Rate, the Catastrophe Frequency and the Rescue Frequency**—Maytansine and its derivatives also suppressed the shortening rate (Table 1). The loss of a GTP-cap at the tips of the growing microtubules leads to rapid shortening (13). Therefore, suppression of the shortening rate and the catastrophe frequency must occur by a cap-stabilizing mechanism. Maytansine, like vinblastine, does not induce GTP-hydrolysis (31). Maytansine is known as a ‘pure inhibitor’ of microtubule



assembly because no alternate polymer structures have been detected (34). Therefore, it is possible that maytansine stabilizes the GTP- (or GDP-Pi) cap since it neither induces detectable alternative lattice structures nor promotes GTP hydrolysis. In addition, the bound drug molecules may stabilize the GTP-bound conformation of tubulin at the microtubule end and thereby inhibit the catastrophe frequency. In addition, maytansine bound at microtubule ends may stabilize the end against shortening by causing a subtle conformational change in the tubulin at the ends.

The rescue frequency was suppressed by all three maytansinoids to approximately equal extents (40–50%). Maytansine is reported to inhibit the GTP exchange of soluble tubulin (31,32). The failure to exchange GTP for GDP at the exchangeable nucleotide site on  $\beta$ -tubulin would result in a shortage of GTP-bound tubulin in the reaction mixture. It is reasonable to suggest that the lack of sufficient GTP-bound tubulin inhibits the regain of the stabilizing cap and thus inhibits rescue.

### Comparison of the Mechanism of Actions of Maytansinoids and Vinblastine

Maytansine is a competitive inhibitor of vincristine binding to tubulin (33). The mechanism of suppression of microtubule dynamics by maytansine and the thiomethyl derivatives has many of the characteristics of the classic end-poisoning mechanism of vinca-domain agents (15), but with some interesting differences. Like vinblastine (35), S-methyl DM1 binds to a few high affinity sites at the ends of the microtubules. However, unlike vinblastine where the dissociation constant for the high affinity binding site is  $\sim 1.9 \mu\text{mol/L}$  (35), the  $K_D$  for S-methyl DM1 binding to the small number of high affinity sites on microtubules is  $0.1 \mu\text{mol/L}$  indicating that it binds to microtubule ends 19-fold more strongly than vinblastine.

Unlike vinca alkaloids (35), neither maytansine nor its derivatives induced formation of spirals at the ends of the microtubules, as we confirmed by electron microscopy. This observation is consistent with previous evidence indicating that maytansine is a potent inhibitor of tubulin aggregation (5,34). However, unlike maytansine, S-methyl DM1 and S-methyl DM4 induced formation of irregular small or large aggregates at higher drug concentrations.

Maytansine at a concentration of  $100 \text{ nmol/L}$  suppressed the growth and shortening rates by 35%, quantitatively similarly to the same concentration of vinblastine (36) (which suppressed the rates by 34% and 47%, respectively). Both compounds suppressed the catastrophe frequency by  $\sim 30\%$ . However, in contrast to vinblastine, which enhanced the rescue frequency ( $\sim 200\%$ ), maytansine and its derivatives suppressed the rescue frequency (40% – 50%). Given that both vinblastine and maytansine share a binding site on tubulin (5), and that both drugs bind at the microtubule tips, their contrasting effects on the rescue frequency are curious. We suggest that these differences may be related, in part, to their different effects on tubulin-GTP hydrolysis and exchange. Only tubulin dimers with beta subunits containing GTP can incorporate into microtubules; continuous replenishment of the beta tubulin GTP, by exchanging GDP with GTP, is necessary for microtubule assembly. Roach and Luduena (37) found that maytansine inhibits the formation of a cross-link between Cys 12 and Cys 201, a characteristic feature of tubulin depleted of exchangeable nucleotide, significantly more strongly than vinblastine (37). The weak effect of vinblastine on tubulin-GTP exchange can be attributed to its inability to make sufficient contact with the C-terminal H6–H7 loop residue Tyr  $\beta 224$  of tubulin (38). In addition, Lin and Hamel (32) found that vinblastine inhibited the rate of GTP hydrolysis twice as strongly as maytansine. Therefore, we propose that vinblastine promotes attainment of a ‘GTP–exchange threshold’ (due to its significantly weaker inhibition of GTP exchange and its lower rate of GTP hydrolysis), which is responsible for vinblastine’s ability to rescue microtubules from rapid shortening. In contrast, by inhibiting replenishment of beta subunit bound GTP, maytansine may inhibit crossing of the ‘GTP–exchange threshold’, thus suppressing rescue.

## Supplementary Material

Refer to Web version on PubMed Central for supplementary material.

## Acknowledgments

**Financial Support:** Supported by NIH grants CA 57291 and NS13560.

We are thankful to Herb Miller for preparation of purified microtubules and to Victor Goldmacher for helpful suggestions.

## Abbreviations

Pipes	1,4-piperazinediethanesulfonic acid
EGTA	ethyleneglycoltetraacetic acid
MTP	tubulin and microtubule associated proteins
MAPs	microtubule associated proteins

## References

1. Kupchan SM, Komoda Y, Branfman AR, et al. The maytansinoids. Isolation, structural elucidation, and chemical interrelation of novel ansa macrolides. *J Org Chem* 1977;42:2349–57. [PubMed: 874612]
2. Kupchan SM, Komoda Y, Court WA, et al. Maytansine, a novel antileukemic ansa macrolide from *Maytenus ovatus*. *J Am Chem Soc* 1972;94:1354–6. [PubMed: 5062169]
3. Remillard S, Rebhun LI, Howie GA, Kupchan SM. Antimitotic activity of the potent tumor inhibitor maytansine. *Science* 1975;189:1002–5. [PubMed: 1241159]
4. Mandelbaum-Shavit F, Wolpert-DeFilippes MK, Johns DG. Binding of maytansine to rat brain tubulin. *Biochem Biophys Res Commun* 1976;72:47–54. [PubMed: 985482]
5. Bhattacharyya B, Wolff J. Maytansine binding to the vinblastine sites of tubulin. *FEBS Lett* 1977;75:159–62. [PubMed: 852577]
6. Cassady JM, Chan KK, Floss HG, Leistner E. Recent developments in the maytansinoid antitumor agents. *Chem Pharm Bull (Tokyo)* 2004;52:1–26. [PubMed: 14709862]
7. Annual Report to the FDA by DCT, NCI, on Maytansine, NSC 153858, IND 11857, February 1984.
8. Helft PR, Schilsky RL, Hoke FJ, et al. A phase I study of cantuzumab mertansine administered as a single intravenous infusion once weekly in patients with advanced solid tumors. *Clin Cancer Res* 2004;10:4363–8. [PubMed: 15240523]
9. Smith SV. Technology evaluation: cantuzumab mertansine, ImmunoGen. *Curr Opin Mol Ther* 2004;6:666–74. [PubMed: 15663331]
10. Erickson HK, Widdison WC, Mayo MF, et al. Tumor delivery and in vivo processing of disulfide-linked and thioether-linked antibody-maytansinoid conjugates. *Bioconjugate Chem* 2010;21:84–92.
11. Kovtun YV, Audette CA, Ye Y, et al. Antibody–drug conjugates designed to eradicate tumors with homogeneous and heterogeneous expression of the target antigen. *Cancer Res* 2006;66:3214–21. [PubMed: 16540673]
12. Krop, I.; LoRusso, P.; Miller, KD., et al. A Phase II Study of Trastuzumab-DM1 (T-DM1), a Novel HER2 Antibody–Drug Conjugate, in patients with HER2+ metastatic breast cancer who were previously treated with an anthracycline, a taxane, Capecitabine, Lapatinib, and Trastuzumab San Antonio Breast Cancer Symposium; 2009; Abstract #710
13. Lopus, M.; Yenjerla, M.; Wilson, L. Microtubule Dynamics. In: Begley, TP., editor. *Encyclopedia of Chemical Biology*. Vol. 3. New Jersey: John Wiley & Sons; 2009. p. 153-160.
14. Jordan MA, Wilson L. Microtubules as a target for anticancer drugs. *Nat Rev Cancer* 2004;4:253–65. [PubMed: 15057285]
15. Jordan MA, Kamath K. How do microtubule–targeted drugs work? An overview *Curr Cancer Drug Targets* 2007;7:730–42.

16. Widdison W, Wilhelm S, Cavanagh E, et al. Semisynthetic Maytansine Analogs for Targeted Treatment of Cancer. *J Med Chem* 2006;49:4392–08. [PubMed: 16821799]
17. Xie H, Audette C, Hoffee M, et al. Pharmacokinetics and biodistribution of the antitumor immunoconjugate, cantuzumab mertansine (huC242-DM1) and its two components in mice. *J Pharm Exp Ther* 2004;308:1073–82.
18. Farrell KW, Wilson L. Tubulin–colchicine complexes differentially poison opposite microtubule ends. *Biochemistry* 1984;23:3741–48. [PubMed: 6477893]
19. Miller HP, Wilson L. Preparation of Microtubule Protein and Purified Tubulin from Bovine Brain by Cycles of Assembly and Disassembly and Phosphocellulose Chromatography. *Methods Cell Biol* 2010;95:3–15. [PubMed: 20466126]
20. Bradford MM. A rapid and sensitive method for the quantitation of microgram quantities of proteins utilizing the principle of protein–dye binding. *Anal Biochem* 1976;72:248–54. [PubMed: 942051]
21. Yenjerla M, Lapointe NE, Lopus M, Cox C, Jordan MA, Feinstein SC, Wilson L. The Neuroprotective Peptide NAP Does Not Directly Affect Polymerization or Dynamics of Reconstituted Neural Microtubules. *J Alzheimers Dis* 2010;19:1377–86. [PubMed: 20061604]
22. Yenjerla M, Lopus M, Wilson L. Analysis of Dynamic Instability of Steady-State Microtubules In Vitro by Video-Enhanced Differential Interference Contrast Microscopy. *Methods Cell Biol* 2010;95:189–202. [PubMed: 20466136]
23. Walker RA, O'Brien ET, Pryer NK, et al. Dynamic instability of individual microtubules analyzed by video light microscopy: rate constants and transition frequencies. *J Cell Biol* 1998;107:1437–48. [PubMed: 3170635]
24. Aneja R, Vangapandu SN, Lopus M, Panda D, Chandra R, Joshi HC. Development of a novel nitro-derivative of noscapine for the potential treatment of drug-resistant ovarian cancer and T-cell lymphoma. *Mol Pharmacol* 2006;69:1801–09. [PubMed: 16517755]
25. Jordan MA, Ojima I, Rosas F, et al. Effects of novel taxanes SB-T-1213 and IDN5109 on tubulin polymerization and mitosis. *Chem Biol* 2002;9:93–101. [PubMed: 11841942]
26. Rosenthal H. E (1967) A graphic method for the determination and presentation of binding parameters in a complex system. *Analyt Biochem* 1967;20:525–32. [PubMed: 6048188]
27. Smith JA, Wilson L, Azarenko O, Zhu X, Lewis BM, Littlefield BA, Jordan MA. Eribulin Binds at Microtubule Ends to a Single Site on Tubulin to Suppress Dynamic Instability. *Biochemistry* 2010;49:1331–7. [PubMed: 20030375]
28. Wilson L, Jordan MA, Morse A, Margolis RL. Interaction of vinblastine with steady state microtubules in vitro. *J Mol Biol* 1982;159:125–49. [PubMed: 7131559]
29. Jordan MA, Walker D, de Arruda M, Barlozzari T, Panda D. Suppression of microtubule dynamics by binding of cemadotin to tubulin: possible mechanism for its antitumor action. *Biochemistry* 1998;37:17571–8. [PubMed: 9860873]
30. Panda D, Dajjo JE, Jordan MA, Wilson L. Kinetic stabilization of microtubule dynamics at steady state in vitro by substoichiometric concentrations of tubulin–colchicine complex. *Biochemistry* 1995;34:9921–9. [PubMed: 7632691]
31. Correia JJ. Effects of antimetabolic agents on tubulin-nucleotide interactions. *Pharmacol Ther* 1991;52:127–47. [PubMed: 1818332]
32. Lin CM, Hamel E. Effects of inhibitors of tubulin polymerization on GTP hydrolysis. *J Biol Chem* 1981;256:9242–5. [PubMed: 6114958]
33. York J, Wolpert-DeFilippes MK, Johns DG, Sethi VS. Binding of maytansinoids to tubulin. *Biochem Pharmacol* 1981;30:3239–43. [PubMed: 7317106]
34. Fellous A, Ludueña RF, Prasad V, et al. Effects of Tau and MAP2 on the interaction of maytansine with tubulin: inhibitory effect of maytansine on vinblastine-induced aggregation of tubulin. *Cancer Res* 1985;45:5004–10. [PubMed: 3928146]
35. Singer WD, Jordan MA, Wilson L, Himes RH. Binding of vinblastine to stabilized microtubules. *Mol Pharmacol* 1989;36:366–70. [PubMed: 2571072]
36. Panda D, Jordan MA, Chu KC, Wilson L. Differential effects of vinblastine on polymerization and dynamics at opposite microtubule ends. *J Biol Chem* 1996;271:29807–12. [PubMed: 8939919]
37. Roach MC, Ludueña RF. Different effects of tubulin ligands on the intrachain cross-linking of beta 1-tubulin. *J Biol Chem* 1984;259:12063–71. [PubMed: 6480599]

38. Cormier A, Marchand M, Ravelli RB, Knossow M, Gigant B. Structural insight into the inhibition of tubulin by vinca domain peptide ligands. *EMBO Rep* 2008;9:1101–6. [PubMed: 18787557]

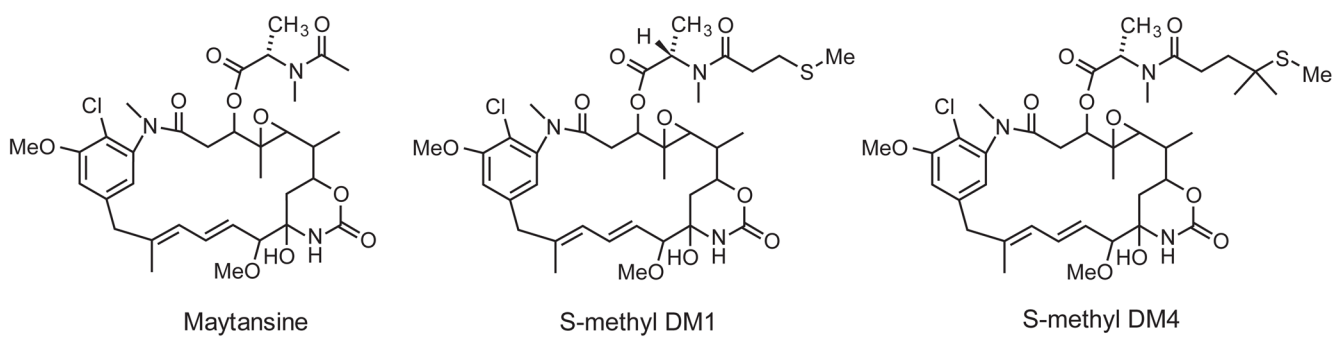


**Figure 1.**  
Structures of maytansine and the maytansine thiomethyl analogs S-methyl DM1 and S-methyl DM4.

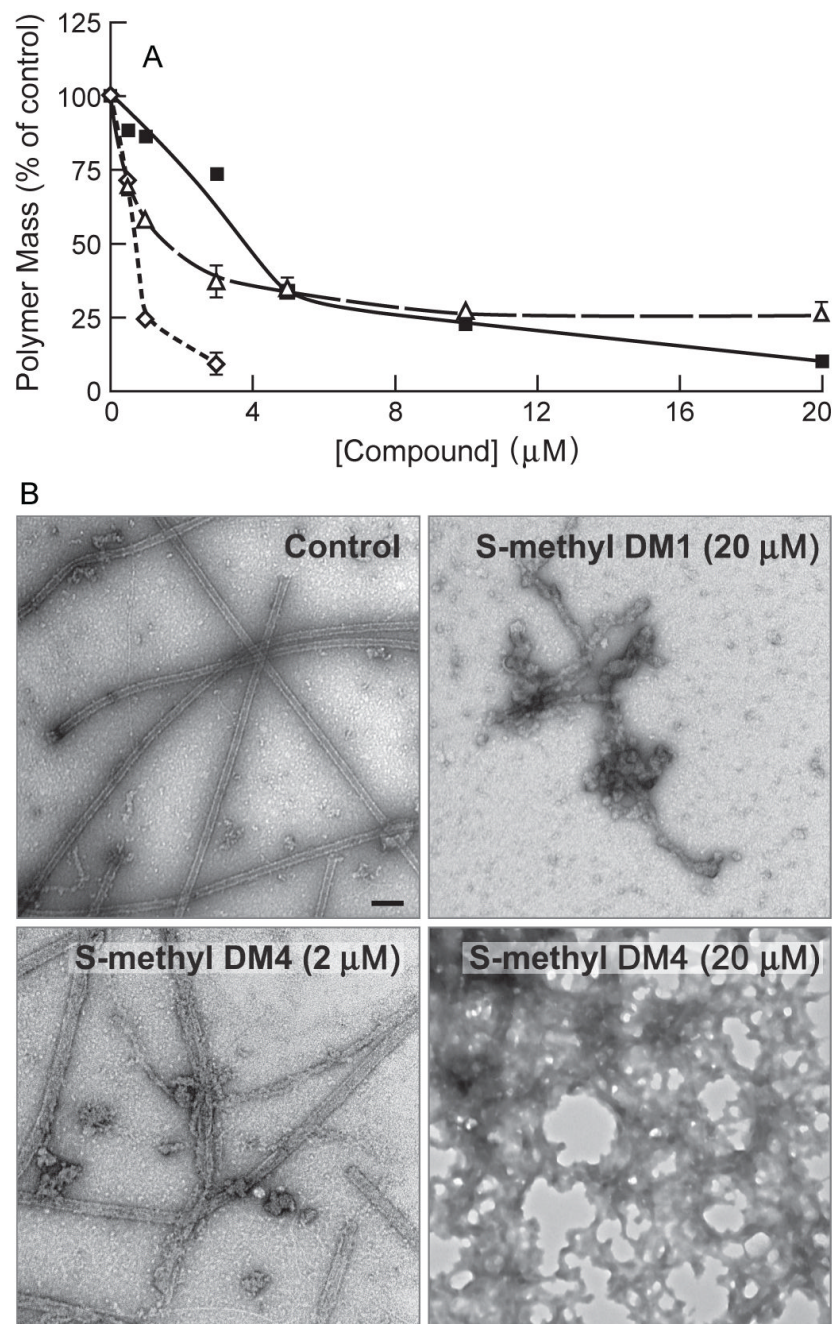


**Figure 2.** Concentration-dependence for inhibition of microtubule assembly by the maytansinoids. **A.** Microtubule protein (3 mg/mL) was assembled in the absence or presence of maytansine (◇), S-methyl DM1 (■), and S-methyl DM4 (△) in the presence of 1 mmol/L GTP in PEM buffer at 30 °C for 45 min. The microtubules were collected by centrifugation (35000 × g, 1 h, 30 °C) and the amount of sedimented protein was determined. Maytansine, S-methyl DM1, S-methyl DM4 inhibited MT assembly with IC<sub>50</sub>'s of 1 ± 0.02 µmol/L, 4 ± 0.1 µmol/L, and 1.7 ± 0.4 µmol/L, respectively. Mean and SD of two experiments. **B.** Electron micrographs of microtubules treated with vehicle (DMSO), S-methyl DM1, or S-methyl DM4. S-methyl DM1

showed few aggregates where as S-methyl DM4 induced extensive aggregation. Images are 100000 × magnifications.

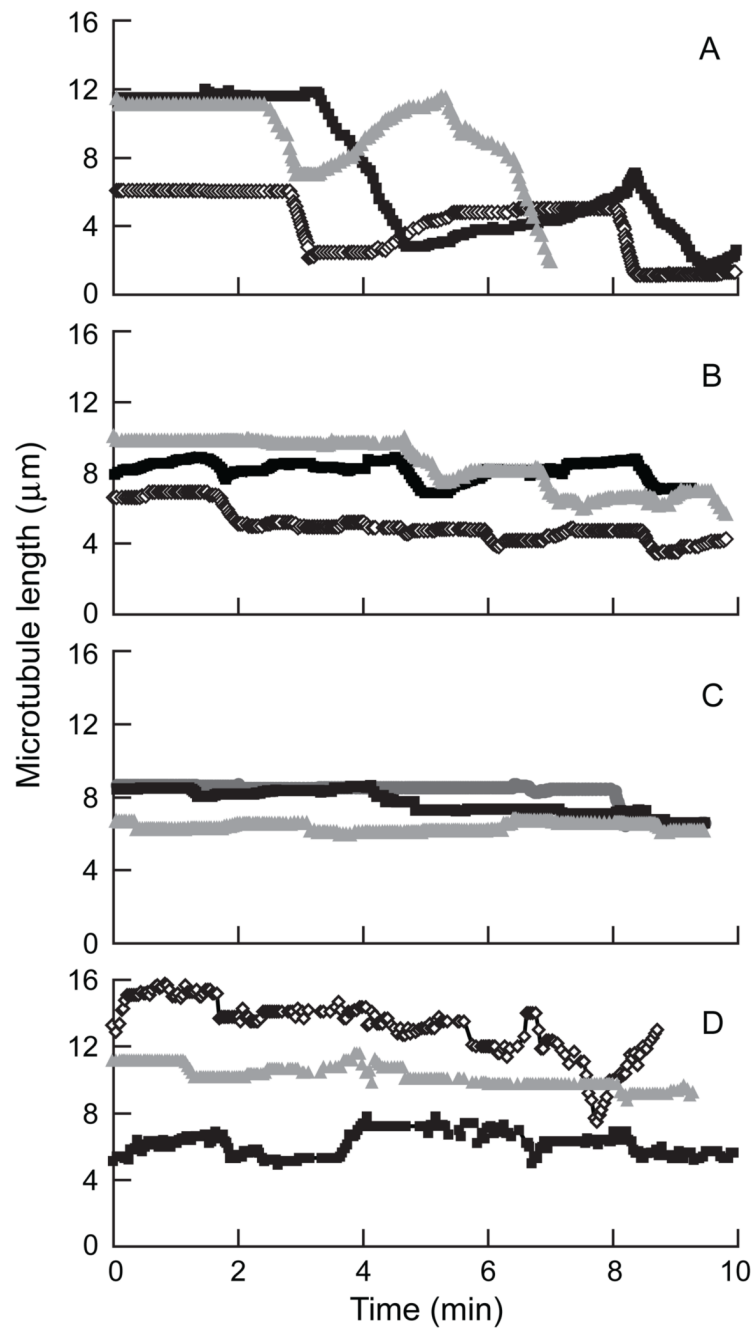


**Figure 3.** Effect of maytansinoids on microtubule dynamic instability. Life history plots of changes in microtubule length at steady state in the absence and presence of 100 nmol/L compound. A, control; B, maytansine; C, S-methyl DM1; and D, S-methyl DM4.



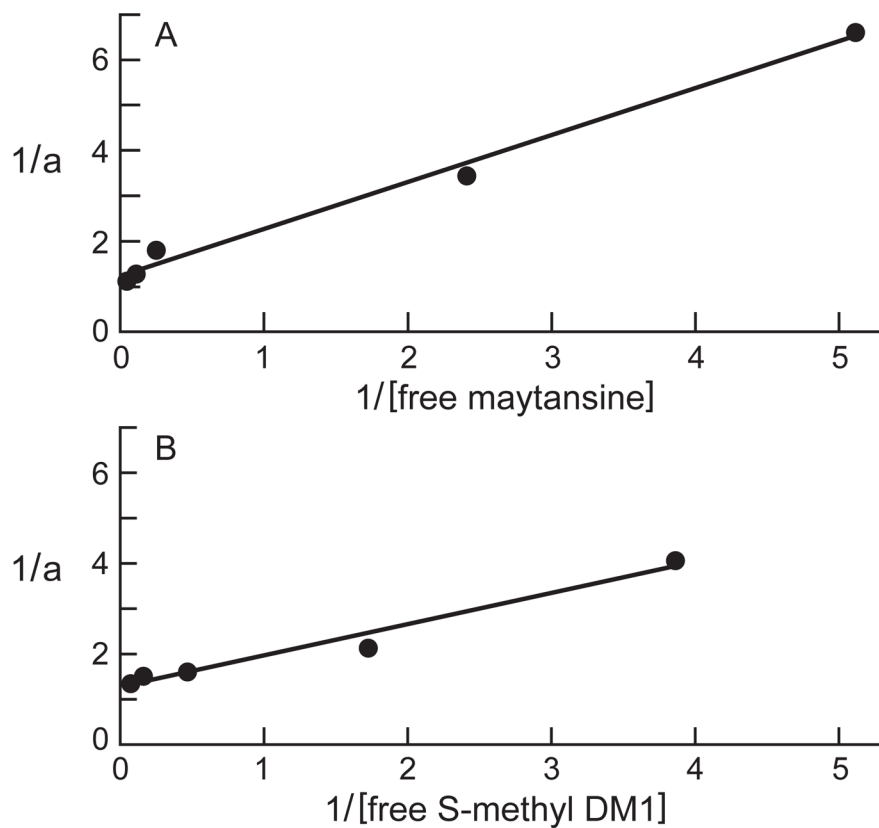


**Figure 4.**

Binding of maytansine (A) or S-methyl DM1 (B) to tubulin. Maytansine (0.5–20  $\mu\text{mol/L}$ ) or S-methyl DM1 (1–8  $\mu\text{mol/L}$ ) was incubated with 3  $\mu\text{mol/L}$  tubulin in PEM buffer for 45 min at 30  $^{\circ}\text{C}$ . The relative intrinsic fluorescence intensity of tubulin was monitored as described in ‘Materials and Methods’. The plot indicates a dissociation constant ( $K_D$ ) of  $0.86 \pm 0.23 \mu\text{mol/L}$  for maytansine (A) and of  $0.93 \pm 0.22 \mu\text{mol/L}$  for S-methyl DM1 (B). The Y-axis shows the inverse of the fractional receptor occupancy (a) of compound and the X-axis shows the inverse of free maytansinoid concentration.

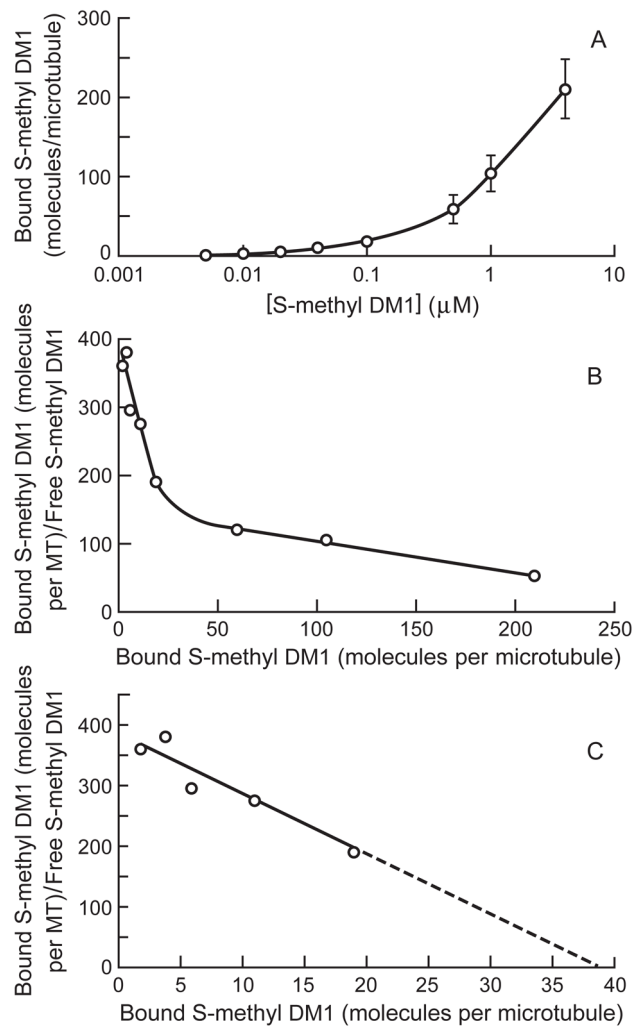


**Figure 5.** Concentration-dependence for binding of S-methyl DM1 to microtubules. **A.** S-methyl DM1 binds to microtubules in a concentration-dependent manner. The graph represents mean and SEM of three independent experiments **B.** Scatchard plot showing binding to both the high affinity and low affinity sites on microtubules. Microtubules were assembled to steady-state (MTP, 3 mg/mL) and then incubated with [ $^3\text{H}$ ]-S-methyl DM1 for 1 h. Microtubules were collected by centrifugation through a glycerol/DMSO cushion. From microtubule lengths, sedimented protein, and incorporated radioactivity, the stoichiometry of the binding of S-methyl DM1 per microtubule was determined. **C.** Scatchard plot showing binding at low drug concentrations and indicating that there are 37 high affinity sites at microtubule ends,  $K_D$  of  $0.1 \pm 0.05 \mu\text{mol/L}$ .

**Table 1**  
Effects of maytansine, S-methyl DMI1, and S-methyl DM4 on microtubule dynamic instability.

Microtubule Dynamic Parameters	Control	Maytansine (0.1 μmol/L)	Percent Change	S-methyl DMI1 (0.1 μmol/L)	Percent Change	S-methyl DM4 (0.1 μmol/L)	Percent Change
Growing Rates (μm/min)	1.7 ± 0.2	1.1 ± 0.2*	35 (-)	1.3 ± 0.4	24 (-)	1.3 ± 0.3	24 (-)
Shortening Rates (μm/min)	8.9 ± 0.8	5.8 ± 0.5*	35 (-)	2.7 ± 0.9**	70 (-)	3.9 ± 0.4**	56 (-)
Percent Time Growing	23.2	24	3.4 (+)	7.3	70 (-)	15.2	34 (-)
Percent Time Shortening	14.8	11	26 (-)	5.4	64 (-)	4.2	72 (-)
Percent Time Attenuated	62	65	5 (+)	87.4	41 (+)	80.6	30 (+)
Growing Lengths (μm/event)	1.9 ± 0.2	1.2 ± 0.1**	37 (-)	1 ± 0.1*	47 (-)	1.6 ± 0.1	16 (-)
Shortening Lengths (μm/event)	3 ± 0.2	1.8 ± 0.9**	40 (-)	1.2 ± 0.2***	60 (-)	1.2 ± 0.2***	60 (-)
Catastrophe Frequency (per min)	0.30	0.21	30 (-)	0.03	90 (-)	0.03	90 (-)
Rescue Frequency (per min)	1.00	0.60	40 (-)	0.56	44 (-)	0.50	50 (-)
Dynamicsity	1.3	0.72	45 (-)	0.21	84 (-)	0.35	73 (-)

Tubulin was polymerized to steady state with axoneme seeds in the presence of 100 nmol/L maytansinoid and the dynamic instability parameters were determined (Materials and Methods).

\*, \*\*, \*\*\* represent significance of differences at > 0.05, > 0.01, > 0.001, respectively, as observed in a Students' t-test with respect to control. 15–25 microtubules were measured for each drug concentration. Data are mean ± SEM.